Eidgenössische Technische Hochschule Zürich
Ecole polytechnique fédérale de Zurich
Politecnico federale di Zurigo
Swiss Federal Institute of Technology Zurich

Mixed *hp*-finite element approximations on geometric edge and boundary layer meshes in three dimensions

A. Toselli and C. Schwab

Research Report No. 2001-02
February 2001

revised

Seminar für Angewandte Mathematik
Eidgenössische Technische Hochschule
CH-8092 Zürich
Switzerland

Mixed hp-finite element approximations on geometric edge and boundary layer meshes in three dimensions

A. Toselli and C. Schwab

Seminar für Angewandte Mathematik
Eidgenössische Technische Hochschule
CH-8092 Zürich
Switzerland

Research Report No. 2001-02 February 2001

revised

Abstract

In this paper, we consider the Stokes problem in a three-dimensional polyhedral domain discretized with hp finite elements of type $\mathbb{Q}^k$ for the velocity and $\mathbb{Q}^{k-2}$ for the pressure, defined on hexahedral meshes anisotropically and non quasi-uniformly refined towards faces, edges, and corners. The inf-sup constant of the discretized problem is independent of arbitrarily large aspect ratios and exhibits the same dependence on k as in in the case of isotropically refined meshes. Our work generalizes a recent result for two-dimensional problems in [8, 9].

Keywords: Mixed methods, hp finite elements, spectral elements, anisotropic meshes

Subject Classification: 65N30, 65N35, 65N12

1 Introduction

It is well–known that solutions of elliptic boundary value problems in polyhedral domains have corner and edge singularities. In addition, boundary layers may also arise in flows with large Reynolds numbers at faces, edges, and corners. Suitably graded meshes, geometrically refined towards corners, edges, and/or faces, are required in order to achieve an exponential rate of convergence of hp finite element approximations; see, e.g., [2, 3, 6, 11, 12].

The Stokes and Navier–Stokes equations are mixed elliptic systems with saddle point variational form. The stability and accuracy of the corresponding finite element approximations depend on an inf–sup condition for the finite element spaces chosen for the velocity and the pressure fields. Even for stable velocity–pressure combinations, the corresponding inf–sup constants may in general be very sensitive to the aspect ratio of the mesh, thus degrading the stability if very thin elements are employed, as required for boundary–layer and singularity resolution. It has recently been shown in the two–dimensional case, for corner and boundary–layer tensor–product meshes, that the inf–sup constant of certain velocity/pressure space pairs for the Stokes problem retains the same dependence on the polynomial degree as for isotropically refined triangulations, independently of arbitrarily large aspect ratios of the mesh; see [11, 8, 9, 1]. Analogous results in three dimensional domains appear to be lacking.

In this paper, we prove that, for the most widely used $\mathbb{Q}^k$–$\mathbb{Q}^{k-2}$ spaces on geometric boundary layer and edge meshes consisting of hexahedral elements in $\mathbb{R}^3$, the inf–sup constant decreases as Ck^{-1}, with a constant C that depends only on the mesh grading factor, but is independent of the degree k, the level of refinement, and arbitrarily large element aspect ratios. We note that this dependence on k is optimal; see [4, §25].

This paper is organized as follows:
In Section 2, we introduce the continuous problem and the finite element spaces for its discretization. They are built on geometric boundary layer and edge meshes, described and constructed in Section 3. In Section 4, we describe the macro–element technique that we repeatedly employ in our proofs. The stability of face, edge, and corner patches for geometric boundary layer meshes is proven in Sections 5, 6, and 7, respectively. The case of geometric edge meshes is treated in Section 8.

2 Problem setting

Let $\Omega \subset \mathbb{R}^3$ be a bounded polyhedral domain. Given a vector $f \in L^2(\Omega)^3$, we consider the following problem: find a velocity $u \in H_0^1(\Omega)^3$ and a pressure $p \in L_0^2(\Omega)$, such that

$$\begin{array}{lcll} \nu(\nabla u, \nabla v)_\Omega - (p, \nabla \cdot v)_\Omega & = & (f, v)_\Omega, & v \in V := H_0^1(\Omega)^3, \\ (q, \nabla \cdot u)_\Omega & = & 0, & q \in M := L_0^2(\Omega). \end{array} \tag{1}$$

Here, $L^2_0(\Omega)$ denotes the subspace of $L^2(\Omega)$ of functions with vanishing mean value in Ω and, for $\mathcal{D} \subseteq \mathbb{R}^3$, $(u,v)_{\mathcal{D}}$ denotes the scalar product in $L^2(\Omega)$ or $L^2(\Omega)^3$.

In order to approximate (1), we replace the continuous spaces $V \times M$ by two finite element spaces $V_N \times M_N \subset V \times M$. Let $(u_N, p_N) \in V_N \times M_N$ be the solution of the corresponding discrete problem:

$$\begin{array}{rcll} \nu(\nabla u_N, \nabla v_N)_\Omega - (p_N, \nabla \cdot v_N)_\Omega &=& (f, v_N)_\Omega, & v_N \in V_N, \\ (q_N, \nabla \cdot u_N)_\Omega &=& 0, & q_N \in M_N. \end{array} \tag{2}$$

A crucial role in the analysis and approximation of (1) is played by the inf–sup condition

$$\inf_{0 \neq p \in L^2_0(\Omega)} \sup_{0 \neq v \in H^1_0(\Omega)^3} \frac{(\nabla \cdot v, p)_\Omega}{|v|_{1,\Omega}\, \|p\|_{0,\Omega}} \geq \gamma > 0, \tag{3}$$

which ensures its well–posedness. The corresponding discrete inf–sup condition for the finite element spaces (V_N, M_N) (also referred to as divergence stability) ensures the well–posedness and quasi–optimality of (2). Indeed, if a stability condition (3) holds for the discrete velocity and pressure spaces, with a constant γ_N, then (2) has a unique solution, and the following error estimates hold

$$\begin{array}{rcl} \|u - u_N\|_{1,\Omega} &\leq& C\gamma_N^{-1} E_V(u,N) + C\nu^{-1} E_P(p,N), \\ \|p - p_N\|_{0,\Omega} &\leq& C\gamma_N^{-2} E_V(u,N) + C\gamma_N^{-1} E_P(p,N), \end{array}$$

where

$$\begin{array}{rcl} E_V(u,N) &:=& \inf_{v \in V_N} \|u - v\|_{1,\Omega}, \\ E_P(p,N) &:=& \inf_{q \in M_N} \|p - q\|_{0,\Omega}, \end{array}$$

are the best approximation errors of the solution (u,p) of (1); see, e.g., [5].

We now specify a particular choice of finite element spaces. Given an affine hexahedral mesh $\mathcal{T}$ and a polynomial degree $k \geq 2$, in order to discretize (1), we consider the following finite element spaces:

$$\begin{array}{rcl} V_N = S_0^{k,1}(\Omega;\mathcal{T})^3 &:=& \left\{u \in H^1_0(\Omega)^3 \mid \ u_{|K} \in \mathbb{Q}_k(K)^3\right\}, \\ M_N = S_0^{k-2,0}(\Omega;\mathcal{T}) &:=& \left\{p \in L^2_0(\Omega) \mid \ p_{|K} \in \mathbb{Q}_{k-2}(K)\right\}. \end{array} \tag{4}$$

Here $\mathbb{Q}_k(K)$ is the space of polynomials of maximum degree k in each variable on K. The mesh $\mathcal{T}$ is said to be *regular* if it is geometrically conforming, or *irregular* if hanging nodes are present; see, e.g., [9, 10]. These spaces are also known as $\mathbb{P}_k$–$\mathbb{P}_{k-2}$ in the spectral element literature. In the following, we also use the polynomial spaces $\mathbb{Q}_{r,s,m}$ of polynomials of degree r, s, and m in the first, second, and third variable, respectively.

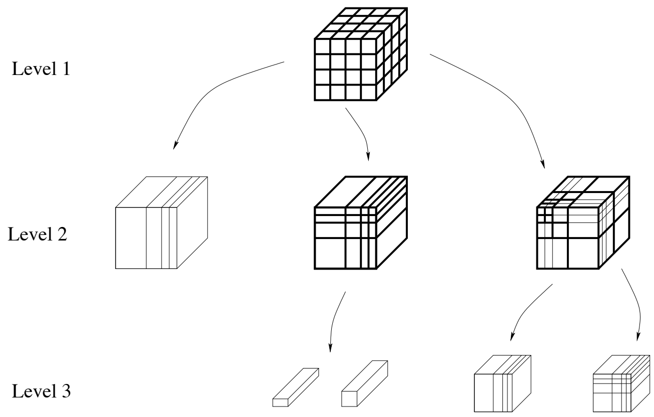

Figure 1: Hierarchic structure of a boundary layer mesh.

3 Geometric meshes

In order to resolve boundary layers and/or singularities, geometrically graded meshes can be employed. They are determined by a mesh grading factor $\sigma \in (0,1)$ and the number of layers n, the thinnest layer having width proportional to σ^n. Robust exponential convergence of hp finite element approximations is achieved if n is suitably chosen. For singularity resolution, n is required to be proportional to the polynomial degree k; see [2, 3]. For boundary layers, the width of the thinnest layer needs to be comparable to that of the boundary layer; see [6, 11, 12]. In practical applications, for boundary layers of fixed size, and edge and corner singularities, n is usually chosen proportional to the polynomial degree k, with the assumption that k is sufficiently large.

3.1 Construction of geometric boundary layer meshes

A geometric boundary layer mesh $\mathcal{T}_{bl}^{n,\sigma}$ is, roughly speaking, the tensor product of meshes that are geometrically refined towards the faces. Figure 1 shows the construction of a geometric boundary layer mesh $\mathcal{T}_{bl}^{n,\sigma}$.

The mesh $\mathcal{T}_{bl}^{n,\sigma}$ is built by first considering an initial shape–regular macro–triangulation $\mathcal{T}_m$ which is successively refined. This process is illustrated in Figure 1. Every macro–element can be refined isotropically (not shown) or anisotropically in order to obtain so–called face, edge, or corner patches (Figure

1, level 2). Here and in the following, we only consider patches obtained by triangulating the reference cube $\hat{Q} := I^3$, with $I := (-1, 1)$. A patch for an element $K \in \mathcal{T}_m$ is obtained by using an affine mapping $F_K : \hat{Q} \to K$. The stability properties proven for patches on the reference cube are equally valid for an arbitrary shape–regular element $K \in \mathcal{T}_m$, with a constant that is independent of the diameter of K.

A **face patch** is given by an anisotropic triangulation of the form

$$\mathcal{T}_f := \{K_x \times I \times I \mid \quad K_x \in \mathcal{T}_x\}, \tag{5}$$

where $\mathcal{T}_x$ is a mesh of $I := (-1, 1)$, geometrically refined towards, say $x = 1$, with grading factor $\sigma \in (0, 1)$ and total number of layers n; see Figure 1 (level 2, left).

An **edge patch** $\mathcal{T}_e$ is given by

$$\mathcal{T}_e := \{K_{xy} \times I \mid \quad K_{xy} \in \mathcal{T}_{xy}\}, \tag{6}$$

where $\mathcal{T}_{xy}$ is a triangulation of $\hat{S} := I^2$ obtained by first considering an irregular corner mesh, geometrically refined towards a vertex of $\hat{S}$, say $(x, y) = (1, 1)$, with grading factor σ and n refinement levels (see Figure 2, level 2, left). The elements of this macro–mesh are then anisotropically refined towards the two edges $x = 1$ and $y = 1$, in order to obtain a regular mesh $\mathcal{T}_{xy}$. We refer to Figure 1 (level 2, center) for an example.

In order to build a **corner patch** $\mathcal{T}_c$, we first consider an initial, irregular, corner mesh $\mathcal{T}_{c,m}$, geometrically refined towards a vertex of $\hat{Q}$, say $(x, y, z) = (1, 1, 1)$, with grading factor σ and n refinement levels; see the mesh in bold lines in Figure 1 (level 2, right). The elements of this macro–mesh are then anisotropically refined towards the three faces $x = 1$, $y = 1$, and $z = 1$ in order to obtain a regular mesh $\mathcal{T}_c$.

Assuming that $n = O(k)$, the number of elements in a face, edge, and corner patch is $O(k)$, $O(k^2)$, and $O(k^3)$, respectively. Consequently, the corresponding FE spaces have $O(k^4)$, $O(k^5)$, and $O(k^6)$ degrees of freedom.

Our main result is the following theorem; see [7, 8, 9] for the corresponding two–dimensional result.

Theorem 3.1 *Let $\mathcal{T} = \mathcal{T}_{bl}^{n,\sigma}$ be a geometric boundary layer mesh. Then, there exists a constant C, that depends on the grading factor σ, but is independent of k, n, and the aspect ratio of $\mathcal{T}$, such that, for any n and $k \geq 2$,*

$$\inf_{0 \neq p \in S_0^{k-2,0}(\Omega,\mathcal{T})} \sup_{0 \neq v \in S_0^{k,1}(\Omega,\mathcal{T})^3} \frac{(\nabla \cdot v, p)_\Omega}{|v|_{1,\Omega} \, \|p\|_{0,\Omega}} \geq C k^{-1}. \tag{7}$$

3.2 Construction of geometric edge meshes

When only singularities and no boundary layers are present (as, e.g., in Stokes flows or in nearly incompressible elasticity), it is not necessary to refine geometrically towards the faces. The corresponding geometric edge meshes $\mathcal{T}_{edge}^{n,\sigma}$

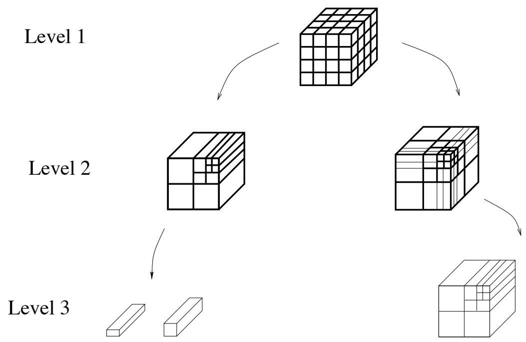

Figure 2: Hierarchic structure of a geometric edge mesh $\mathcal{T}^{n,\sigma}_{edge}$.

are tensor products of meshes that are geometrically refined towards the edges only. Figure 2 shows the construction of a geometric edge mesh $\mathcal{T}^{n,\sigma}_{edge}$.

As in the case of a boundary layer mesh, $\mathcal{T}^{n,\sigma}_{edge}$ is built by first considering an initial shape–regular macro–triangulation $\mathcal{T}_m$ which is successively refined. This process is illustrated in Figure 2. Every macro–element can be refined isotropically (not shown) or anisotropically in order to obtain so–called edge or corner patches (Figure 2, level 2).

An **edge patch** $\mathcal{T}_e$ is given by

$$\mathcal{T}_e := \{K_{xy} \times I \mid \quad K_{xy} \in \mathcal{T}_{xy}\}, \tag{8}$$

where $\mathcal{T}_{xy}$ is an irregular corner mesh, geometrically refined towards a vertex of $\hat{S}$ with grading factor σ and n refinement levels; see Figure 2 (level 2, left).

In order to build a **corner patch** $\mathcal{T}_c$, we first consider an initial, irregular, corner mesh $\mathcal{T}_{c,m}$, geometrically refined towards a vertex of $\hat{Q}$, with grading factor σ and n refinement levels; see the mesh in bold lines in Figure 2 (level 2, right). The elements of this macro–mesh are then refined towards the three edges adjacent to the vertex. We note that the macro–mesh $\mathcal{T}_{c,m}$ is the same as for a boundary layer mesh, but $\mathcal{T}_c$ is in general irregular. Figure 3 shows the difference between corner patches for boundary layer and edge meshes.

Assuming $n = O(k)$, one can show that the number of elements in an edge and a corner patch is $O(k)$ and $O(k^2)$, respectively. Consequently, the corresponding FE spaces have $O(k^3)$ and $O(k^5)$ degrees of freedom; see [3].

In section 8, we show that Theorem 3.1 also holds for an edge mesh $\mathcal{T} = \mathcal{T}^{n,\sigma}_{edge}$.

Figure 3: Geometrically refined corner patches for boundary layer (left) and edge (right) meshes.

4 Macro–element technique

In order to prove Theorem 3.1, we repeatedly use a macro–element technique; see [13, 14, 7, 9]. Given a mesh $\mathcal{T}$, it is enough to prove the divergence–stability for a couple of low dimensional spaces, typically $S_0^{2,1}(\Omega,\mathcal{T})^3$ and $S_0^{0,0}(\Omega,\mathcal{T})$, on a macro-mesh contained in or coinciding with $\mathcal{T}$, and the stability of local higher order spaces defined on the single elements K of the macro-mesh, $S_0^{k,1}(K)^3$ and $S_0^{k-2,0}(K)$ in this case.

The following theorem holds. We refer to [13, 14, 7, 9] for a proof.

Theorem 4.1 *Let $\mathcal{F}$ be a family of irregular or regular affine meshes on the reference element $\hat{Q}$. On a bounded polyhedral domain $\Omega \subset \mathbb{R}^3$, let $\mathcal{T}$ be an affine mesh which is obtained from a (coarser) affine shape–regular macro-element mesh $\mathcal{T}_m$ in the following way: Some elements of $\mathcal{T}_m$ are further partitioned into $F_K(\hat{\mathcal{T}})$ where $\hat{\mathcal{T}} \in \mathcal{F}$ and F_K is the affine mapping between $\hat{Q}$ and K. Let $k \geq 2$ be a polynomial degree. Assume that there exists a space $X_N \subseteq S_0^{k,1}(\Omega,\mathcal{T})^3 \subset H_0^1(\Omega)^3$ such that*

$$\inf_{0\neq p\in S_0^{0,0}(\Omega,\mathcal{T}_m)} \sup_{0\neq v\in X_N} \frac{(\nabla\cdot v,p)_\Omega}{|v|_{1,\Omega}\,\|p\|_{0,\Omega}} \geq C_1, \tag{9}$$

with a constant $C_1 > 0$ independent of k. Assume that on the reference element $\hat{Q}$ the local stability condition

$$\inf_{0\neq p\in S_0^{k-2,0}(\hat{Q})} \sup_{0\neq v\in S_0^{k,1}(\hat{Q})^3} \frac{(\nabla\cdot v,p)_{\hat{Q}}}{|v|_{1,\hat{Q}}\|p\|_{0,\hat{Q}}} \geq C_2\,k^{-1}, \qquad \forall k\geq 2, \tag{10}$$

is valid with $C_2 > 0$ independent of k. Assume further that the family $\mathcal{F}$ is *uniformly stable in the sense that there holds*

$$\inf_{0\neq p\in S_0^{k-2,0}(\hat{Q},\hat{\mathcal{T}})} \sup_{0\neq v\in S_0^{k,1}(\hat{Q},\hat{\mathcal{T}})^3} \frac{(\nabla\cdot v,p)_{\hat{Q}}}{|v|_{1,\hat{K}}\|p\|_{0,\hat{Q}}} \geq C_2\, k^{-1}, \tag{11}$$

for all $\hat{\mathcal{T}}\in\mathcal{F}$ *and all* k.

Then, there exists a constant $C>0$ *only depending on* C_1 *and* C_2*, such that the spaces* $S_0^{k,1}(\Omega,\mathcal{T})^3$ *and* $S_0^{k-2,0}(\Omega,\mathcal{T})$ *satisfy (7). The constant* C *can be bounded by*

$$C\geq \tilde{C}\,\frac{C_2}{\kappa^3}\,\min\{1,C_1^2\},$$

where κ *is the aspect ratio of the elements of* $\mathcal{T}_m$ *and* $\tilde{C}$ *is independent of* k, κ, C_1*, and* C_2.

We note that we apply the macro–element technique recursively in our analysis. This is illustrated in Figure 1. At the top level, we have the shape–regular macro–mesh $\mathcal{T}_m$, which is successively refined. Every macro–element can be refined isotropically (not shown), or anisotropically towards a face (second level, left), or an edge (second level, center), or a corner (second level, right). The divergence stability for the shape–regular macro–mesh at the top level and the isotropically refined patches is well–known; see [14]. We then prove the stability of the single patches for the higher order spaces:

- **Face patch**. We build a Fortin operator, generalizing the analysis in [8, Sect. 3].
- **Edge patch**. We use a macro–element technique. The corresponding macro–mesh is displayed in bold lines in 1 (second level, center) and we use the two–dimensional result for low order spaces defined on corner patches. We then prove the local stability for the higher order spaces on the single stretched elements (third level, center) using a Fortin operator.
- **Corner patch**. For the corner patch, we generalize the two–dimensional analysis in [9, Sect. 4]. We prove the stability for low order spaces on the corner mesh in bold lines in Figure 1 (second level, right) and then use the stability of the other patches. We note that the refined elements of this macro-mesh are face and edge patches.

5 Face patches

A face patch is given by a mesh $\mathcal{T}_f$ of the form (5). For this patch, we prove that the inf–sup constant γ_N is independent of $\mathcal{T}_x$ and, consequently, of σ and n.

In this section, we generalize the analysis in [8, Sect. 3] for boundary layer patches in two–dimensions, by building a Fortin operator $\Pi_k : H_0^1(\hat{Q})^3 \longrightarrow S_0^{k,1}(\hat{Q}, \mathcal{T}_f)$, that satisfies the following property.

Theorem 5.1 *There exists a constant C, independent of k and the diameter and the aspect ratio of $\mathcal{T}_f$, such that, for all $v \in H_0^1(\hat{Q})^3$,*

$$|\Pi_k v|_{1,\hat{Q}} \leq Ck|v|_{1,\hat{Q}}, \tag{12}$$

$$(\nabla \cdot v, p)_{\hat{Q}} = (\nabla \cdot \Pi_k v, p)_{\hat{Q}}, \quad p \in S_0^{k-2,0}(\hat{Q}, \mathcal{T}_f). \tag{13}$$

It is then immediate to see that if the inf–sup condition (3) for the continuous spaces $H_0^1(\hat{Q})^3$–$L_0^2(\hat{Q})$ holds and a Fortin operator Π_k that satisfies Theorem 5.1 can be found, the following inf–sup condition for the discrete spaces holds

$$\inf_{0 \neq p \in S_0^{k-2,0}(\hat{Q}, \mathcal{T}_f)} \sup_{0 \neq v \in S_0^{k,1}(\hat{Q}, \mathcal{T}_f)^3} \frac{(\nabla \cdot v, p)_{\hat{Q}}}{|v|_{1,\hat{Q}} \|p\|_{0,\hat{Q}}} \geq Ck^{-1}, \tag{14}$$

with a constant C that is independent of k and the diameter and the aspect ratio of $\mathcal{T}_f$.

5.1 The Fortin operator for the face patch

We begin by defining an operator on the reference cube $\hat{Q}$. We first need to define some of the geometric objects of $\hat{Q}$:
Let the faces of $\hat{Q}$ perpendicular to the x–axis be

$$\Gamma_{\pm}^{x} := \{x = \pm 1\} \times (-1, 1)^2.$$

The two other sets of faces $\Gamma_{\pm}^{i}$, $i = y, z$, are defined in a similar way. The edges of $\hat{Q}$ parallel to the x, y, and z–axis are denoted by E_j^x, E_j^y, and E_j^z, $j = 1, \ldots, 4$, respectively. Finally, let $\{P_i, \quad i = 1, \cdots, 8\}$ be the set of vertices of $\hat{Q}$. Similar definitions hold for an element $K \in \mathcal{T}_f$.

Definition 5.1 *Let $r, s, m \geq 2$ and $v \in H^{\epsilon+3/2}(\hat{Q})$, $\epsilon > 0$. We define $u = I_{r,s,m} v$ as the unique polynomial in $\mathbb{Q}_{r,s,m}(\hat{Q})$ satisfying the following $(r+1)(s+1)(m+1)$ conditions:*

$$u(P_i) = v(P_i), \quad i = 1, \ldots, 8, \tag{15}$$

$$\int_{E_i^x} (u - v) p \, dx = 0, \quad p \in \mathbb{Q}_{r-2}, \quad i = 1, \ldots, 4, \tag{16}$$

$$\int_{E_i^y} (u - v) p \, dy = 0, \quad p \in \mathbb{Q}_{s-2}, \quad i = 1, \ldots, 4, \tag{17}$$

$$\int_{E_i^z} (u - v) p \, dz = 0, \quad p \in \mathbb{Q}_{m-2}, \quad i = 1, \ldots, 4, \tag{18}$$

$$\int_{\Gamma^x_\pm} (u-v)p\,dydz = 0, \quad p \in \mathbb{Q}_{s-2,m-2}, \tag{19}$$

$$\int_{\Gamma^y_\pm} (u-v)p\,dxdz = 0, \quad p \in \mathbb{Q}_{r-2,m-2}, \tag{20}$$

$$\int_{\Gamma^z_\pm} (u-v)p\,dxdy = 0, \quad p \in \mathbb{Q}_{r-2,s-2}, \tag{21}$$

$$\int_{\hat{Q}} (u-v)p\,dxdydz = 0, \quad p \in \mathbb{Q}_{r-2,s-2,m-2}. \tag{22}$$

We note that $I_{r,s,m}$ cannot be defined on the whole space $H^1(\hat{Q})$ since values at the edges or vertices of $\partial\hat{Q}$ are not defined in general. However, it can be defined on the space

$$H(\hat{Q}) := \{v \in H^1(\hat{Q}) \mid \quad v = 0 \text{ on } \Gamma^y_\pm \text{ and } \Gamma^z_\pm\}.$$

In this case, v can be assumed to be zero on $\partial\hat{Q} \setminus (\Gamma^x_- \cup \Gamma^x_+)$ in Definition 5.1.

An interpolation operator $I^K_{r,s,m}$ can also be defined on an affinely mapped element $K = F_K(\hat{Q}) \in \mathcal{T}_f$, for functions in $H(K)$. Here, $H(K)$ is defined in a similar way as $H(\hat{Q})$.

Our Fortin operator is then defined locally using the operators $\{I^K_{r,s,m}\}$.

Definition 5.2 *Let $v = (v_x, v_y, v_z) \in H^1_0(\hat{Q})^3$. We define $u = (u_x, u_y, u_z) := \Pi_k v$ as the unique vector in $S^{k,1}_0(\hat{Q}, \mathcal{T}_f)^3$ that satisfies*

$$u_i := I^K_{k,k,k} v_i, \quad \text{on } K,$$

for $i = x, y, z$ and $K \in \mathcal{T}_f$.

Note that Π_k is well defined, since, for $v \in H^1_0(\hat{Q})^3$, the restrictions of v_i to $K \in \mathcal{T}_f$, for $i = x, y, z$, belong to $H(K)$.

5.2 Proof of Theorem 5.1

Let $\mathcal{I}(\hat{Q})$ be the set of polynomials on $\hat{Q}$ and $\mathcal{I}_0(\hat{Q})$ its subspace of polynomials that vanish on $\Gamma^y_\pm$ and $\Gamma^z_\pm$.

We will first consider the operator $I_{r,s,m} : \mathcal{I}(\hat{Q}) \longrightarrow \mathbb{Q}_{r,s,m}(\hat{Q})$ and introduce a suitable basis for the two polynomial spaces, which allows a convenient representation of $I_{r,s,m}$.

Let $\{L_i(x),\ i \in \mathbb{N}_0\}$ be the set of Legendre polynomials of degree i on I. We also set $L_{-1} = L_{-2} = 0$. We consider the one–dimensional basis $\{U_i(x),\ i \in \mathbb{N}_0\}$ defined by

$$\begin{aligned} &U_0(x) = 1, \quad U_1(x) = x, \\ &U_i(x) = \int_{-1}^{x} L_{i-1}(t)dt, \quad i \geq 2. \end{aligned} \tag{23}$$

The set $\{U_i(x)U_j(y)U_l(z);\ i,j,l \in \mathbb{N}_0\}$ is thus a basis for $\mathcal{I}(\hat{Q})$. Indeed, each $v \in \mathcal{I}(\hat{Q})$ can be uniquely written as

$$v(x,y,z) = \sum_{i=0}^{\infty}\sum_{j=0}^{\infty}\sum_{l=0}^{\infty} a_{ijl} U_i(x)U_j(y)U_l(z), \tag{24}$$

where only finitely many terms are non–vanishing. For a polynomial $v \in \mathbb{Q}_{r,s,m}(\hat{Q})$ the sum is taken for $i \le r$, $j \le s$, $l \le m$.

We recall that, if $\gamma_i := \frac{1}{2i+1}$, $i \in \mathbb{N}_0$, with $\gamma_{-1} = 1$ and $\gamma_{-2} = 0$, we have

$$\int_I L_i(x)L_j(x)dx = 2\gamma_i\delta_{ij}, \tag{25}$$

and

$$U_i(x) = \gamma_{i-1}\left(L_i(x) - L_{i-1}(x)\right), \quad i \in \mathbb{N}_0. \tag{26}$$

In addition, using (23), (25), and (26), we can show the identities

$$\int_I U_i(x)U_j(x)dx = \begin{cases} 2\gamma_{i-1}^2\gamma_i, & j = i = 0,1, \\ 2\gamma_{i-1}^2(\gamma_i + \gamma_{i-2}), & j = i \ge 2, \\ -2\gamma_{i-1}\gamma_i\gamma_{i+1}, & j = i+2,\ i \ge 0, \\ -2\gamma_{i-3}\gamma_{i-2}\gamma_{i-1}, & j = i-2,\ i \ge 2, \\ 0, & \text{otherwise}. \end{cases} \tag{27}$$

Lemma 5.1 *Let $v \in \mathcal{I}(\hat{Q})$ be written in the form (24). Then*

$$\begin{aligned} \|v_x\|_{0,\hat{Q}}^2 &= \sum_{i=1}^{\infty}\sum_{j,l=0}^{\infty} 8\,\gamma_{i-1}\gamma_j\gamma_l\left((\gamma_{j-1}\gamma_{l-1}a_{i,j,l} - \gamma_{j-1}\gamma_{l+1}a_{i,j,l+2})\right. \\ &- \left.(\gamma_{j+1}\gamma_{l-1}a_{i,j+2,l} - \gamma_{j+1}\gamma_{l+1}a_{i,j+2,l+2})\right)^2, \end{aligned} \tag{28}$$

$$\begin{aligned} \|v_y\|_{0,\Gamma_\pm^x}^2 &:= \|v_y\|_{0,\Gamma_-^x}^2 + \|v_y\|_{0,\Gamma_+^x}^2 \\ &= \sum_{i=0}^{1}\sum_{j=1}^{\infty}\sum_{l=0}^{\infty} 8\,\gamma_{j-1}\gamma_l(\gamma_{l-1}a_{i,j,l} - \gamma_{l+1}a_{i,j,l+2})^2, \end{aligned} \tag{29}$$

$$\begin{aligned} \|v\|_{0,\Gamma_\pm^x}^2 &:= \|v\|_{0,\Gamma_-^x}^2 + \|v\|_{0,\Gamma_+^x}^2 \\ &= \sum_{i=0}^{1}\sum_{j,l=0}^{\infty} 8\,\gamma_j\gamma_l\left((\gamma_{j-1}\gamma_{l-1}a_{i,j,l} - \gamma_{j-1}\gamma_{l+1}a_{i,j,l+2})\right. \\ &- \left.(\gamma_{j+1}\gamma_{l-1}a_{i,j+2,l} - \gamma_{j+1}\gamma_{l+1}a_{i,j+2,l+2})\right)^2. \end{aligned} \tag{30}$$

The corresponding expressions for $\|v_y\|_{0,\hat{Q}}^2$, $\|v_z\|_{0,\hat{Q}}^2$, $\|v_z\|_{0,\Gamma_\pm^x}^2$, and for the norms on the other faces are obtained by permutations of the indices.

Proof. The proof of (28) can be carried out in a similar way as in the two–dimensional case (see [8]) and as in the simpler case where $v \in \mathcal{I}(\hat{Q}) \cap H_0^1(\hat{Q})$ (see [14]).

For (29), it is enough to realize that the restriction of v to a face, e.g., $x = 1$,

$$v(1, y, z) = \sum_{i=0}^{1} \sum_{j=1}^{\infty} \sum_{l=0}^{\infty} a_{ijl} U_i(1) U_j(y) U_l(z),$$

is a polynomial in y and z. The expressions for the L^2–norm of the derivatives of a polynomial in two variables proven in [8, Lem. 3.14], can be thus employed. The proof of (30) can be carried out in a similar way as for (28). □

Lemma 5.2 *Let $v \in \mathcal{I}(\hat{Q})$ be written in the form (24). Then*

$$u(x, y, z) = (I_{r,s,m} v)(x, y, z) = \sum_{i=0}^{r} \sum_{j=0}^{s} \sum_{l=0}^{m} a_{ijl} U_i(x) U_j(y) U_l(z).$$

Proof. Let

$$u(x, y, z) = \sum_{i=0}^{r} \sum_{j=0}^{s} \sum_{l=0}^{m} b_{ijl} U_i(x) U_j(y) U_l(z).$$

We first note that the only contributions that do not vanish on the boundary in the expansions of v and u are for $0 \le i \le 1$ or $0 \le j \le 1$ or $0 \le l \le 1$.

Condition (15) ensures that

$$b_{ijl} = a_{ijl}, \quad 0 \le i, j, l \le 1, \tag{31}$$

since $u - v$ vanishes at the vertices of $\hat{Q}$.

We next consider condition (16), with $p(x) = L'_{n-1}(x)$, $n = 2, \ldots, r$, and the edge

$$E_1^x = \{(x, y, z), \quad x \in I,\ y = -1,\ z = -1\}.$$

We have

$$\sum_{i=0}^{r} (b_{i00} - b_{i01} - b_{i10} + b_{i11}) \int_I U_i L'_{n-1} dx = \sum_{i=0}^{\infty} (a_{i00} - a_{i01} - a_{i10} + a_{i11}) \int_I U_i L'_{n-1} dx.$$

Integrating by parts and using (31), we obtain

$$b_{n00} - b_{n01} - b_{n10} + b_{n11} = a_{n00} - a_{n01} - a_{n10} + a_{n11}, \quad n = 2, \ldots, r.$$

Using (16) for the remaining edges, we obtain the four conditions, for $n = 2, \ldots, r$,

$$(b_{n00} - a_{n00}) \pm (b_{n01} - a_{n01}) \pm (b_{n10} - a_{n10}) + (b_{n11} - a_{n11}) = 0,$$

and finally

$$b_{nij} = a_{nij}, \quad 2 \le n \le r, \quad 0 \le i, j \le 1. \tag{32}$$

Using (17) and (18), we find, in a similar way,

$$\begin{aligned} b_{inj} &= a_{inj}, \quad 2 \le n \le s, \quad 0 \le i, j \le 1, &(33)\\ b_{ijn} &= a_{ijn}, \quad 2 \le n \le m, \quad 0 \le i, j \le 1. &(34)\end{aligned}$$

We next consider condition (19), with

$$p(y,z) = L'_{n-1}(y)L'_{q-1}(z), \quad n = 2, \ldots, s, \quad q = 2, \ldots, m,$$

and the face Γ^x_-. We have

$$\begin{aligned} &\sum_{j=0}^{s}\sum_{l=0}^{m}(b_{0jl} - b_{1jl}) \int_I U_j L'_{n-1} dy \int_I U_l L'_{q-1} dz \\ &= \sum_{j=0}^{\infty}\sum_{l=0}^{\infty}(a_{0jl} - a_{1jl}) \int_I U_j L'_{n-1} dy \int_I U_l L'_{q-1} dz. \end{aligned}$$

Integrating by parts and using (31), (32), (33), and (34), we obtain

$$(b_{0nq} - b_{1nq}) - (a_{0nq} - a_{1nq}) = 0, \quad n = 2, \ldots, s, \quad q = 2, \ldots, m.$$

Using then (16) for Γ^x_+, we obtain the two conditions, for $n = 2, \ldots, s$ and $q = 2, \ldots, m$,

$$(b_{0nq} - a_{0nq}) \pm (b_{1nq} - a_{1nq}) = 0,$$

and finally

$$b_{inq} = a_{inq}, \quad 2 \le n \le s, \quad 2 \le q \le m, \quad 0 \le i \le 1. \tag{35}$$

Using (20) and (21), we find, in a similar way,

$$(36)$$

$$\begin{aligned} b_{niq} &= a_{niq}, \quad 2 \le n \le r, \quad 2 \le q \le m, \quad 0 \le i \le 1, &(37)\\ b_{nqi} &= a_{nqi}, \quad 2 \le n \le r, \quad 2 \le q \le s, \quad 0 \le i \le 1. &(38)\end{aligned}$$

We finally consider condition (22), with

$$p(x,y,z) = L'_{n-1}(x)L'_{q-1}(y)L'_{t-1}(z), \quad 2 \le n \le r,\ 2 \le q \le s,\ 2 \le t \le m.$$

We have

$$\begin{aligned} &\sum_{i=0}^{r}\sum_{j=0}^{s}\sum_{l=0}^{m} b_{ijl} \int_I U_i L'_{n-1} dx \int_I U_j L'_{q-1} dy \int_I U_l L'_{t-1} dz \\ &= \sum_{i=0}^{\infty}\sum_{j=0}^{\infty}\sum_{l=0}^{\infty} a_{ijl} \int_I U_i L'_{n-1} dx \int_I U_j L'_{q-1} dy \int_I U_l L'_{t-1} dz. \end{aligned}$$

Integrating by parts and using the previously proven conditions, we obtain

$$b_{nqt} = a_{nqt}, \quad 2 \le n \le r,\ 2 \le q \le s,\ 2 \le t \le m,$$

which concludes the proof □

Lemma 5.3 *Let $v \in \mathcal{I}_0(\hat{Q})$ be written in the form (24) and $u := I_{r,s,m}v$. Then*

$$\begin{aligned} \|u_x\|^2_{0,\hat{Q}} &\le C\, sm\, \|v_x\|^2_{0,\hat{Q}}, &(39)\\ \|u_y\|^2_{0,\hat{Q}} &\le C\, rm\, \|v_y\|^2_{0,\hat{Q}} + C\, m\, S_y, &(40)\\ \|u_z\|^2_{0,\hat{Q}} &\le C\, rs\, \|v_z\|^2_{0,\hat{Q}} + C\, s\, S_z, &(41)\end{aligned}$$

where

$$\begin{aligned} S_y &:= \sum_{i=0}^{1}\sum_{j=1}^{s}\sum_{l=0}^{m-2} 4\gamma_{r-1}\gamma_{j-1}\gamma_l(\gamma_{l-1}a_{ijl} - \gamma_{l+1}a_{i,j,l+2})^2,\\ S_z &:= \sum_{i=0}^{1}\sum_{j=0}^{s-1}\sum_{l=1}^{m} 4\gamma_{r-1}\gamma_j\gamma_{l-1}(\gamma_{j-1}a_{ijl} - \gamma_{j+1}a_{i,j+2,l})^2.\end{aligned}$$

Proof. We will first prove a bound for u_x in case $v \in \mathcal{I}(\hat{Q})$. Using Lemma 5.2 and (28), we see that the sums in (28) can be decomposed into four parts

$$\begin{aligned}\|u_x\|^2_{0,\hat{Q}} = \sum_{i=1}^{r}\sum_{j=0}^{s-2}\sum_{l=0}^{m-2} + \sum_{i=1}^{r}\sum_{j=0}^{s-2}\sum_{l=m-1}^{m} &+ \sum_{i=1}^{r}\sum_{j=s-1}^{s}\sum_{l=0}^{m-2} + \sum_{i=1}^{r}\sum_{j=s-1}^{s}\sum_{l=m-1}^{m}\\ &= A + B_1 + B_2 + D.\end{aligned}$$

Using (28), we immediately have

$$A \le \|v_x\|^2_{0,\hat{Q}}.$$

We next consider B_1 and note that B_1 consists of just two terms in l, for $l = m-1$ and $l = m$. We first consider the term for $l = m$ and suppose that m is odd. We can write, for i and j fixed,

$$\begin{aligned} &(\gamma_{j-1}\gamma_{m-1}a_{ijm} - \gamma_{j+1}\gamma_{m-1}a_{i,j+2,m})\\ &= \sum_{l=0}^{\frac{m-3}{2}} [-(\gamma_{j-1}\gamma_{2l}a_{i,j,2l+1} - \gamma_{j+1}\gamma_{2l}a_{i,j+2,2l+1})\\ &+ (\gamma_{j-1}\gamma_{2l+2}a_{i,j,2l+3} - \gamma_{j+1}\gamma_{2l+2}a_{i,j+2,2l+3})]\\ &+ (\gamma_{j-1}a_{i,j,1} - \gamma_{j+1}a_{i,j+2,1}).\end{aligned}$$

Taking the square of both sides, we obtain

$$\begin{aligned}
&(\gamma_{j-1}\gamma_{m-1}a_{ijm} - \gamma_{j+1}\gamma_{m-1}a_{i,j+2,m})^2 \\
\leq\ & (m-1)\sum_{l=0}^{\frac{m-3}{2}} [-(\gamma_{j-1}\gamma_{2l}a_{i,j,2l+1} - \gamma_{j+1}\gamma_{2l}a_{i,j+2,2l+1}) \\
+\ & (\gamma_{j-1}\gamma_{2l+2}a_{i,j,2l+3} - \gamma_{j+1}\gamma_{2l+2}a_{i,j+2,2l+3})]^2 \\
+\ & 2(\gamma_{j-1}a_{i,j,1} - \gamma_{j+1}a_{i,j+2,1})^2.
\end{aligned}$$

The term for $l = m-1$ can be bounded in a similar way: for odd m, we obtain

$$\begin{aligned}
&(\gamma_{j-1}\gamma_{m-2}a_{i,j,m-1} - \gamma_{j+1}\gamma_{m-2}a_{i,j+2,m-1})^2 \\
\leq\ & (m-1)\sum_{l=0}^{\frac{m-3}{2}} [-(\gamma_{j-1}\gamma_{2l-1}a_{i,j,2l} - \gamma_{j+1}\gamma_{2l-1}a_{i,j+2,2l}) \\
+\ & (\gamma_{j-1}\gamma_{2l+1}a_{i,j,2l+2} - \gamma_{j+1}\gamma_{2l+1}a_{i,j+2,2l+2})]^2 \\
+\ & 2(\gamma_{j-1}a_{i,j,0} - \gamma_{j+1}a_{i,j+2,0})^2.
\end{aligned}$$

Analogous expressions can be found for even m. Using (28), we obtain

$$B_1 \leq Cm\|v_x\|^2_{0,\hat{Q}} + C\sum_{i=1}^{r}\sum_{j=0}^{s-2}\sum_{l=0}^{1} 4\gamma_{i-1}\gamma_j\gamma_{m-1}(\gamma_{j-1}a_{i,j,l} - \gamma_{j+1}a_{i,j+2,l})^2.$$

In a similar way, we also find

$$B_2 \leq Cs\|v_x\|^2_{0,\hat{Q}} + C\sum_{i=1}^{r}\sum_{j=0}^{1}\sum_{l=0}^{m-2} 4\gamma_{i-1}\gamma_{s-1}\gamma_l(\gamma_{l-1}a_{i,j,l} - \gamma_{l+1}a_{i,j,l+2})^2.$$

We finally consider the last term D and note that D consists of four terms in j and l, for $j = s-1, s$ and $l = m-1, m$, which can be bounded as before, by employing one telescoping series for j and one for l. We obtain

$$\begin{aligned}
D \leq\ & Csm\|v_x\|^2_{0,\hat{Q}} \\
+\ & Cm\sum_{i=1}^{r}\sum_{j=0}^{1}\sum_{l=0}^{m-2} 4\gamma_{i-1}\gamma_{s-1}\gamma_l(\gamma_{l-1}a_{i,j,l} - \gamma_{l+1}a_{i,j,l+2})^2 \\
+\ & Cs\sum_{i=1}^{r}\sum_{j=0}^{s-2}\sum_{l=0}^{1} 4\gamma_{i-1}\gamma_j\gamma_{m-1}(\gamma_{j-1}a_{i,j,l} - \gamma_{j+1}a_{i,j+2,l})^2 \\
+\ & C\sum_{i=1}^{r}\sum_{j=0}^{1}\sum_{l=0}^{1} 4\gamma_{i-1}\gamma_{m-1}\gamma_{s-1}a^2_{i,j,l}.
\end{aligned}$$

We note that the corresponding bounds for u_y and u_z can be found by permutations of the indices. Inequality (39) can be found by noticing that, if $v \in \mathcal{I}_0(\hat{Q})$, we have

$$a_{ijl} = 0, \quad 0 \le j \le 1 \quad \text{or} \quad 0 \le l \le 1.$$

Inequalities (40) and (41) can be found in a similar way. □

Lemma 5.4 *Let $v \in \mathcal{I}_0(\hat{Q})$ and $u := I_{r,s,m}v$. Then*

$$\begin{aligned}
\|u_y\|^2_{0,\hat{Q}} &\le C\,rm\,\|v_y\|^2_{0,\hat{Q}} + C\,\frac{m}{r}\,\|v_y\|^2_{0,\Gamma^x_\pm}, && (42)\\
\|u_z\|^2_{0,\hat{Q}} &\le C\,rs\,\|v_z\|^2_{0,\hat{Q}} + C\,\frac{s}{r}\,\|v_z\|^2_{0,\Gamma^x_\pm}, && (43)\\
\|u_y\|^2_{0,\hat{Q}} &\le C\,rm\,\|v_y\|^2_{0,\hat{Q}} + C\,\frac{ms^4}{r}\,\|v\|^2_{0,\Gamma^x_\pm}, && (44)\\
\|u_z\|^2_{0,\hat{Q}} &\le C\,rs\,\|v_z\|^2_{0,\hat{Q}} + C\,\frac{sm^4}{r}\,\|v\|^2_{0,\Gamma^x_\pm}, && (45)\\
\|u_y\|^2_{0,\hat{Q}} &\le C\,rm\,\|v_y\|^2_{0,\hat{Q}} + C\,\frac{ms^2}{r}\,\|v\|^2_{1/2,00,\Gamma^x_\pm}, && (46)\\
\|u_z\|^2_{0,\hat{Q}} &\le C\,rs\,\|v_z\|^2_{0,\hat{Q}} + C\,\frac{sm^2}{r}\,\|v\|^2_{1/2,00,\Gamma^x_\pm}, && (47)
\end{aligned}$$

where

$$\|v\|^2_{1/2,00,\Gamma^x_\pm} := \|v\|^2_{H^{1/2}_{00}(\Gamma^x_-)} + \|v\|^2_{H^{1/2}_{00}(\Gamma^x_+)}.$$

Proof. We only consider the terms in u_y in detail. Those in u_z can be treated in a similar way.

We immediately find (42) by using (29) and noting that $\gamma_{r-1} \le C/r$.

In order to prove (44), we need to bound

$$\begin{aligned}
S_y &= \sum_{i=0}^{1}\sum_{j=1}^{s}\sum_{l=0}^{m-2} 4\gamma_{r-1}\gamma_{j-1}\gamma_l(\gamma_{l-1}a_{ijl} - \gamma_{l+1}a_{i,j,l+2})^2\\
&= \sum_{j=1}^{s}\sum_{l=0}^{m-2} 4\gamma_{r-1}\gamma_{j-1}\gamma_l(\gamma_{l-1}a_{0jl} - \gamma_{l+1}a_{0,j,l+2})^2\\
&+ \sum_{j=1}^{s}\sum_{l=0}^{m-2} 4\gamma_{r-1}\gamma_{j-1}\gamma_l(\gamma_{l-1}a_{1jl} - \gamma_{l+1}a_{1,j,l+2})^2\\
&=: S_0 + S_1.
\end{aligned}$$

We first consider S_0. Recalling that $\gamma_{s-1} \le \gamma_{j-1}$, for $j \le s$, we can write

$$S_0 \le 4\frac{\gamma_{r-1}}{\gamma_{s-1}}\sum_{l=0}^{m-2}\gamma_l\sum_{j=1}^{s}\gamma^2_{j-1}(\gamma_{l-1}a_{0jl} - \gamma_{l+1}a_{0,j,l+2})^2. \tag{48}$$

We next set, for a fixed l,

$$A_j := \gamma_{j-1}(\gamma_{l-1}a_{0jl} - \gamma_{l+1}a_{0,j,l+2}),$$

and denote $J = J(l) \leq s$ the index j such that

$$A_J^2 = \max_{0 \leq j \leq s} \{A_j^2\}.$$

We first assume that J is even. If $A_J^2 > 0$, then $J \geq 2$ since $a_{ijl} = 0$ for $0 \leq j \leq 1$. Noting that $A_0 = 0$, we can then write

$$A_J = -\sum_{j=0}^{\frac{J-2}{2}} (A_{2j} - A_{2j+2}),$$

and bound A_J^2 by

$$\begin{aligned} A_J^2 \leq \frac{J}{2} \sum_{j=0}^{\frac{J-2}{2}} &[(\gamma_{2j-1}\gamma_{l-1}a_{0,2j,l} - \gamma_{2j-1}\gamma_{l+1}a_{0,2j,l+2}) \\ - \quad &(\gamma_{2j+1}\gamma_{l-1}a_{0,2j+2,l} - \gamma_{2j+1}\gamma_{l+1}a_{0,2j+2,l+2})]^2. \end{aligned}$$

Using this bound and (48), we find

$$\begin{aligned} S_0 &\leq 4\frac{\gamma_{r-1}}{\gamma_{s-1}} \sum_{l=0}^{m-2} \gamma_l \, s \, A_{J(l)}^2 \\ &\leq \quad 4\frac{\gamma_{r-1}}{\gamma_{s-1}} \sum_{l=0}^{m-2} \gamma_l \, s \frac{J}{2} \sum_{j=0}^{\frac{J-2}{2}} [(\gamma_{2j-1}\gamma_{l-1}a_{0,2j,l} - \gamma_{2j-1}\gamma_{l+1}a_{0,2j,l+2}) \\ &- \quad (\gamma_{2j+1}\gamma_{l-1}a_{0,2j+2,l} - \gamma_{2j+1}\gamma_{l+1}a_{0,2j+2,l+2})]^2 \\ &\leq \quad 2\frac{\gamma_{r-1}}{\gamma_s^2} \sum_{l=0}^{m-2} \gamma_l \, s^2 \sum_{j=0}^{\infty} \gamma_j [(\gamma_{j-1}\gamma_{l-1}a_{0,j,l} - \gamma_{j-1}\gamma_{l+1}a_{0,j,l+2}) \\ &- \quad (\gamma_{j+1}\gamma_{l-1}a_{0,j+2,l} - \gamma_{j+1}\gamma_{l+1}a_{0,j+2,l+2})]^2, \end{aligned}$$

and, using (30),

$$S_0 \leq C\frac{s^4}{r} \, \|v\|_{0,\Gamma_{\pm}^x}^2.$$

We note that, in case $A_J^2 = 0$, this bound trivially holds. The case of J odd can be treated in a similar way.

Using a similar bound for S_1, we find (44).

Using now (42), (44), and an interpolation argument between the spaces $L^2(\Gamma_-^x) \times L^2(\Gamma_+^x)$ and $H_0^1(\Gamma_-^x) \times H_0^1(\Gamma_+^x)$, we find (47); see the proof of [8, Th. 3.5] for more details. □

The following corollary is a straightforward consequence of (46), (47), Lemma 5.4, the trace theorem, and the Poincaré inequality.

Corollary 5.1 *Let* $v \in \mathcal{I}_0(\hat{Q})$ *and* $u := I_{r,s,m}v$. *Then*

$$\|u_y\|^2_{0,\hat{Q}} \leq C\, rm\, \|v_y\|^2_{0,\hat{Q}} + C\, \frac{ms^2}{r}\, |v|^2_{1,\hat{Q}}, \tag{49}$$

$$\|u_z\|^2_{0,\hat{Q}} \leq C\, rs\, \|v_z\|^2_{0,\hat{Q}} + C\, \frac{sm^2}{r}\, |v|^2_{1,\hat{Q}}. \tag{50}$$

We are now ready to give a bound for the case of a general element in $\mathcal{T}_f$.

Lemma 5.5 *Let* $v \in H^1(K)$, *with* $K = (x_1, x_2) \times (-1, 1)^2$. *Suppose in addition that* v *vanishes on all* ∂K *except on* Γ^x_- *and* Γ^x_+. *Then there exists a constant* $C > 0$, *independent of* v, r, s, m, *and* K *such that*

$$|I^K_{r,s,m}v|^2_{1,K} \leq C \left(\max\{sm, rm, rs\} + \frac{ms}{r} \max\{s, m\} \right) |v|^2_{1,K}.$$

If, in addition, $r = s = m = k \geq 2$, *then*

$$|I^K_{k,k,k}v|_{1,K} \leq Ck|v|_{1,K}.$$

Proof. We first note that, since $\mathcal{I}_0(\hat{Q})$ is dense in $H(\hat{Q})$, (39), (49), and (50) also hold for $v \in H(\hat{Q})$.

Let now $h := (x_2 - x_1)/2$. Then, $F_K : \hat{Q} \to K$ is given by

$$\begin{bmatrix} x \\ y \\ z \end{bmatrix} = \begin{bmatrix} h\, \hat{x} + \dfrac{x_1 + x_2}{2} \\ \hat{y} \\ \hat{z} \end{bmatrix}.$$

If $\hat{v} := v \circ F_K$, we have

$$\begin{aligned}
\|\hat{v}_{\hat{x}}\|^2_{0,\hat{Q}} &= h\|v_x\|^2_{0,K}, \quad \|(I_{r,s,m}\hat{v})_{\hat{x}}\|^2_{0,\hat{Q}} = h\|(I^K_{r,s,m}v)_x\|^2_{0,K} \\
\|\hat{v}_{\hat{y}}\|^2_{0,\hat{Q}} &= \frac{1}{h}\|v_y\|^2_{0,K}, \quad \|(I_{r,s,m}\hat{v})_{\hat{y}}\|^2_{0,\hat{Q}} = \frac{1}{h}\|(I^K_{r,s,m}v)_y\|^2_{0,K}, \\
\|\hat{v}_{\hat{z}}\|^2_{0,\hat{Q}} &= \frac{1}{h}\|v_z\|^2_{0,K}, \quad \|(I_{r,s,m}\hat{v})_{\hat{z}}\|^2_{0,\hat{Q}} = \frac{1}{h}\|(I^K_{r,s,m}v)_z\|^2_{0,K}.
\end{aligned}$$

In addition, we have

$$|\hat{v}|^2_{1,\hat{Q}} \leq \frac{1}{h}\, |v|^2_{1,K}.$$

Inequalities (39), (49), and (50) then give

$$\begin{aligned}
h\, \|(I^K_{r,s,m}v)_x\|^2_{0,K} &\leq C\, sm\, h\, \|v_x\|^2_{0,K}, \\
h^{-1}\, \|(I^K_{r,s,m}v)_y\|^2_{0,K} &\leq C\, rm\, h^{-1}\, \|v_y\|^2_{0,K} + C\, \frac{ms^2}{r}\, h^{-1}\, |v|^2_{1,K}, \\
h^{-1}\, \|(I^K_{r,s,m}v)_z\|^2_{0,K} &\leq C\, rs\, h^{-1}\, \|v_z\|^2_{0,K} + C\, \frac{sm^2}{r}\, h^{-1}\, |v|^2_{1,K},
\end{aligned}$$

which concludes the proof. □

We are now ready to prove Theorem 5.1:
Inequality (12) is a direct consequence of Lemma 5.5. We then note that, since the pressure space $S_0^{k-2,0}(\hat{Q},\mathcal{T}_f)$ consists of discontinuous functions, it is enough to prove (13) on a single element $K \in \mathcal{T}_f$. Let $p \in S_0^{k-2,0}(\hat{Q},\mathcal{T}_f)$ and $v \in H_0^1(\hat{Q})^3$. We have

$$(\nabla \cdot v, p)_K = -(v, \nabla p)_K + (v \cdot n, p)_{\partial K}.$$

Since ∇p and p are polynomials of degree $k-2$ on K, using the definition of Π_k, we find

$$(\nabla \cdot v, p)_K = -(\Pi_k v, \nabla p)_K + (\Pi_k v \cdot n, p)_{\partial K} = (\nabla \cdot (\Pi_k v), p)_K,$$

which concludes the proof.

We conclude this section by stating a corollary that will be useful to prove the stability of edge patches.

Corollary 5.2 *Let $v \in H_0^1(K)$ and*

$$K = (x_1, x_2) \times (y_1, y_2) \times (z_1, z_2). \tag{51}$$

Then, there exists a constant C, independent of v, r, s, m, and K such that

$$|I^K_{r,s,m} v|^2_{1,K} \leq C \left(\max\{sm, rm, rs\}\right) |v|^2_{1,K}.$$

If in addition $r = s = m = k \geq 2$, then

$$|I^K_{k,k,k} v|_{1,K} \leq Ck|v|_{1,K}.$$

and

$$(\nabla \cdot v, p)_K = (\nabla \cdot I^K_{k,k,k} v, p)_K, \quad p \in S_0^{k-2,0}(K).$$

We note that for $v \in H_0^1(K)$, $I^K_{k,k,k} v$ is the operator introduced in [14].

6 Edge patches

An edge patch is given by a mesh $\mathcal{T}_e$ of the form (6). For this patch, we prove that the inf–sup constant γ_N depends on σ, but is independent of n and the aspect ratio of $\mathcal{T}_e$.

In our analysis, $\mathcal{T}_e$ plays the role of macro–mesh. We first prove the stability for low order spaces defined on $\mathcal{T}_e$, by employing the two–dimensional result for corner patches $\mathcal{T}_{xy}$ in [9, Sect. 4]. Using then Corollary 5.2, which provides a Fortin operator for an element anisotropically stretched along three directions, we prove the stability for higher order spaces on the single elements of $\mathcal{T}_e$.

We first recall the two–dimensional result proven in [9, Sect. 4]: there exists a constant C, depending on σ, but otherwise independent of the number n of layers in the geometric mesh $\mathcal{T}_{xy}$, such that

$$\inf_{0\neq p\in S_0^{0,0}(\hat{S},\mathcal{T}_{xy})} \sup_{0\neq v\in S_0^{2,1}(\hat{S},\mathcal{T}_{xy})^2} \frac{(\nabla\cdot v,p)_{\hat{S}}}{|v|_{1,\hat{S}}\,\|p\|_{0,\hat{S}}} \geq C > 0. \tag{52}$$

Condition (52) is equivalent to the existence of a linear operator

$$\pi_{xy} : S_0^{0,0}(\hat{S},\mathcal{T}_{xy}) \longrightarrow S_0^{2,1}(\hat{S},\mathcal{T}_{xy})^2,$$

such that

$$\begin{array}{rcl} (\nabla_{xy}\cdot(\pi_{xy}p),p)_{\hat{S}} & \geq & C\|p\|^2_{0,\hat{S}}, \\ |\pi_{xy}p|_{1,\hat{S}} & \leq & \|p\|_{0,\hat{S}}. \end{array} \tag{53}$$

We have the following trivial result

Lemma 6.1 *The spaces $S_0^{0,0}(\hat{S},\mathcal{T}_{xy})$ and $S_0^{0,0}(\hat{Q},\mathcal{T}_e)$ are isomorphic. We have*

$$\|p\|^2_{0,\hat{Q}} = 2\,\|p\|^2_{0,\hat{S}},$$

for all $p\in S_0^{0,0}(\hat{Q},\mathcal{T}_e)$. In addition, $p\in S^{0,0}(\hat{Q},\mathcal{T}_e)$ belongs to $S_0^{0,0}(\hat{Q},\mathcal{T}_e)$ if and only if

$$\int_{\hat{S}} p\,dx = 0.$$

We next need to build a low–order velocity space which is stable on $\mathcal{T}_e$. We first decompose a three–dimensional vector $v\in S_0^{2,1}(\hat{Q},\mathcal{T}_e)^3$ into a component in the xy–plane and one along the z–direction:

$$v=(v_{xy},v_z),\quad v_z := v\cdot e_z,\quad v_{xy} := v - v_z\,e_z,$$

with e_z the unit vector parallel to the positive z–direction. We then define an operator $I_V : S_0^{2,1}(\hat{S},\mathcal{T}_{xy})^2 \to S_0^{2,1}(\hat{Q},\mathcal{T}_e)^3$, such that $u=I_V v$ is given by

$$u_{xy}=(1-z^2)v,\quad u_z=0.$$

Let $X_N := \mathit{Range}(I_V)\subset S_0^{2,1}(\hat{Q},\mathcal{T}_e)^3$. We have

Lemma 6.2 *The spaces $S_0^{2,1}(\hat{S},\mathcal{T}_{xy})^2$ and X_N are isomorphic. There exist two constants c_1 and C_2, such that, for $v\in S_0^{2,1}(\hat{S},\mathcal{T}_{xy})^2$,*

$$c_1|v|^2_{1,\hat{S}} \leq |I_V v|^2_{1,\hat{Q}} \leq C_2|v|^2_{1,\hat{S}}.$$

Proof. Let $u = I_V v$, with $v \in S_0^{2,1}(\hat{S}, \mathcal{T}_{xy})^2$. We have

$$|u|^2_{1,\hat{Q}} = \int_I dz \int_{\hat{S}} |\nabla((1-z^2)v(x,y))|^2 dxdy.$$

For the upper bound, we can write

$$\begin{aligned} |u|^2_{1,\hat{Q}} &\leq 2 \int_I dz \int_{\hat{S}} \left((1-z^2)^2 |\nabla_{xy} v|^2 + 4z^2 |v|^2\right) \, dxdy \\ &\leq \; C \int_{\hat{S}} \left(|\nabla_{xy} v|^2 + |v|^2\right) \, dxdy \leq C_2 |v|^2_{1,\hat{S}}, \end{aligned}$$

where, for the last step, we have used the Poincaré inequality for functions in $H_0^1(\hat{S})$. The lower bound can be proven in a similar way. □

We are now ready to prove the following result.

Lemma 6.3 *There exists an operator*

$$\pi : S_0^{0,0}(\hat{Q}, \mathcal{T}_e) \longrightarrow S_0^{2,1}(\hat{Q}, \mathcal{T}_e)^3,$$

such that

$$\begin{aligned} (\nabla \cdot (\pi p), p)_{\hat{Q}} &\geq C \|p\|^2_{0,\hat{Q}}, \\ |\pi p|_{1,\hat{Q}} &\leq \|p\|_{0,\hat{Q}}, \end{aligned} \tag{54}$$

where C depends on σ, but is otherwise independent of n and the aspect ratio of $\mathcal{T}_e$.

Proof. In order to define π, we use the two–dimensional operator π_{xy}. Given $p \in S_0^{0,0}(\hat{Q}, \mathcal{T}_e)$, $u = \pi p \in X_N$ is defined by

$$u := I_V(\pi_{xy} p) = \left((1-z^2)\pi_{xy} p, 0\right).$$

We note that π is well–defined due to Lemma 6.1.

In order to prove the first inequality of (54), we write

$$\begin{aligned} (\nabla \cdot (\pi p), p)_{\hat{Q}} &= \int_I (1-z^2) \, dz \int_{\hat{S}} \nabla_{xy} \cdot (\pi_{xy} p) \, p \, dxdy \\ &= \; \frac{4}{3} (\nabla_{xy} \cdot (\pi_{xy} p), p)_{\hat{S}} \geq C \|p\|^2_{0,\hat{S}} \geq C \|p\|^2_{0,\hat{Q}}, \end{aligned}$$

where we have used (53) and Lemma 6.1.

For the second inequality of (54), we use Lemmas 6.1 and 6.2, and (53), to obtain

$$|\pi p|^2_{1,\hat{Q}} \leq C |\pi_{xy} p|^2_{1,\hat{S}} \leq C \|p\|^2_{0,\hat{S}} \leq C \|p\|^2_{0,\hat{Q}}.$$

□

We are now left with the task of proving the divergence–stability for the spaces $S_0^{k,1}(K)^3$ and $S_0^{k-2,0}(K)$, for $K \in \mathcal{T}_e$.

Lemma 6.4 *There exists a constant C independent of k and the diameter and the aspect ratio of $K \in \mathcal{T}_e$, such that*

$$\inf_{0\neq p\in S_0^{k-2,0}(K)} \sup_{0\neq v\in S_0^{k,1}(K)^3} \frac{(\nabla\cdot v, p)_K}{|v|_{1,K}\,\|p\|_{0,K}} \geq Ck^{-1}.$$

Proof. We first note that every $K \in \mathcal{T}_e$ is of the form (51). The existence of a Fortin operator $I^K_{k,k,k} : H^1_0(K)^3 \to S_0^{k,1}(K)^3$ that satisfies Corollary 5.2 and the inf–sup condition (3) for the continuous spaces ensure that the inf–sup condition for the discrete spaces $S_0^{k,1}(K)^3$–$S_0^{k-2,0}(K)$ holds with a constant γ_N that is bounded from below by Ck^{-1}. □

Lemmas 6.3 and 6.4, and the macro–element technique then allow us to prove the divergence stability of the edge patch.

Theorem 6.1 *Let $\mathcal{T}_e$ be an edge triangulation with grading factor σ and n layers. Then, there exists a constant C, that depends on σ, but is independent of k, n, and the aspect ratio of $\mathcal{T}_e$, such that*

$$\inf_{0\neq p\in S_0^{k-2,0}(\hat{Q},\mathcal{T}_e)} \sup_{0\neq v\in S_0^{k,1}(\hat{Q},\mathcal{T}_e)^3} \frac{(\nabla\cdot v, p)_{\hat{Q}}}{|v|_{1,\hat{Q}}\|p\|_{0,\hat{Q}}} \geq Ck^{-1}. \tag{55}$$

Proof. It is enough to use Theorem 4.1 with $\mathcal{T} = \mathcal{T}_e$ and $\mathcal{T}_m = \mathcal{T}_e$. □

We note that the dependency on the grading factor σ only comes from the constant C in (53). Consequently the constant in Theorem 6.1 has the same dependence on σ as in the two–dimensional case. The analysis in [1] and the numerical tests in [9, Sect. 3.1] show that

$$C = C(\sigma) \geq \tilde{C}\sqrt{\sigma(1-\sigma)}.$$

7 Corner patches

A corner patch is given by a geometric mesh $\mathcal{T}_c$, with grading factor σ and n layers. For this patch, we prove that the inf–sup constant γ_N depends on σ, but is independent of n and the aspect ratio of $\mathcal{T}_c$.

In our analysis, we generalize the result in [9, Sect. 4] for two–dimensional corner patches.

We first need to introduce a low–order velocity space $\mathcal{L}_0^{1,1}(\hat{Q}, \mathcal{T}_{c,m})$ on the corner macro–mesh $\mathcal{T}_{c,m}$.

$$S_0^{1,1}(\hat{Q}, \mathcal{T}_{c,m})^3 \subset \mathcal{L}_0^{1,1}(\hat{Q}, \mathcal{T}_{c,m}) \subset S_0^{2,1}(\hat{Q}, \mathcal{T}_{c,m})^3.$$

Given an element $K \in \mathcal{T}_{c,m}$, such that, $K = F_K(\hat{Q})$, we introduce some notations associated to its faces. Let the faces of $\hat{Q}$ perpendicular to the $\hat{x}$–axis be

$$\begin{aligned} \hat{\Gamma}^x_1 &:= \{\hat{x} = -1\} \times (-1,1)^2, \\ \hat{\Gamma}^x_2 &:= \{\hat{x} = +1\} \times (-1,1)^2. \end{aligned}$$

The two other sets of faces $\hat{\Gamma}_i^j$, for $j = y, z$ and $i = 1, 2$, are defined in a similar way. Let Γ_i^j, for $j = x, y, z$ and $i = 1, 2$, be the corresponding faces of K and $n_{j,i}$ the unit vectors, which are perpendicular to them, pointing outward.

To the two x–faces of $\hat{Q}$, $\hat{\Gamma}_i^x$, $i = 1, 2$, we can associate the two functions

$$\begin{aligned} \hat{q}_{x,1} &:= (1-\hat{x}) \cdot (1+\hat{y})(1-\hat{y}) \cdot (1+\hat{z})(1-\hat{z}), \\ \hat{q}_{x,2} &:= (1+\hat{x}) \cdot (1+\hat{y})(1-\hat{y}) \cdot (1+\hat{z})(1-\hat{z}), \end{aligned}$$

respectively. We note that, $\hat{q}_{x,1}$, for instance, vanishes on all the faces except on $\hat{\Gamma}_1^x$ and, when restricted to this face, is a polynomial in $\mathbb{Q}_2$. The functions $\hat{q}_{j,i}$, for $j = y, z$ and $i = 1, 2$, associated to the other faces can be defined in a similar way by suitable permutations of the indices.

We now define, for $j = x, y, z$ and $i = 1, 2$, the vector functions

$$w_{j,i} := n_{j,i} \left(\hat{q}_{j,i} \circ F_K^{-1} \right) \in \mathbb{Q}_2(K)^3,$$

and the local space

$$\mathcal{L}^1(K) := \mathbb{Q}_1(K)^3 \oplus span\{w_{j,i}; \quad j = x, y, z;\ i = 1, 2\}.$$

The corresponding global space is

$$\mathcal{L}_0^{1,1}(\hat{Q}, \mathcal{T}_{c,m}) = \mathcal{L}_0^{1,1}(\hat{Q}) := \left\{ v \in H_0^1(\hat{Q})^3 | \quad v_{|K} \in \mathcal{L}^1(K),\ K \in \mathcal{T}_{c,m} \right\}.$$

Before proving the divergence stability for the low–order spaces $\mathcal{L}_0^{1,1}(\hat{Q}, \mathcal{T}_{c,m})$ and $S_0^{0,0}(\hat{Q}, \mathcal{T}_{c,m})$, we need to introduce a Clément–type interpolation operator for the three–dimensional irregular mesh $\mathcal{T}_{c,m}$. We begin by introducing some notations for the corner macro-mesh $\mathcal{T}_{c,m} = \mathcal{T}_{c,m}^{n,\sigma}$, refined towards a vertex, e.g., $V = (1, 1, 1)$.

The corner macro–mesh $\mathcal{T}_{c,m}^{n,\sigma}$ can be constructed recursively. This is illustrated in Figure 4. Let $\mathcal{T}_{c,m}^{0,\sigma} = \hat{Q}$. Then, $\mathcal{T}_{c,m}^{1,\sigma}$ is obtained by partitioning $\mathcal{T}_{c,m}^{0,\sigma}$ into eight elements by dividing its sides in a σ:$(1-\sigma)$ ratio. Let

$$\mathcal{T}_{c,m}^{1,\sigma} = \{\Omega_{i,1},\ 1 \leq i \leq 8\},$$

with $\Omega_{8,1}$ denoting the element that contains V. At the next refinement level $l = 2$, we partition $\Omega_{8,1}$ into eight parallelepipeds in a similar way. The final mesh $\mathcal{T}_{c,m}^{n,\sigma}$ is obtained after $l = n$ refinement steps. At an intermediate refinement level $1 \leq l \leq n-1$, there are seven new parallelepipeds introduced at level l that do not touch V:

$$\{\Omega_{i,l},\ 1 \leq i \leq 7\}, \quad 1 \leq l \leq n-1.$$

For $l = n$, let

$$\{\Omega_{i,n},\ 1 \leq i \leq 8\},$$

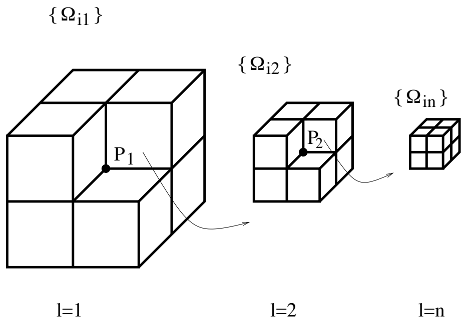

Figure 4: Recursive construction of an irregular corner mesh $\mathcal{T}_{c,m}$.

be the new eight parallelepipeds obtained after the last refinement. We remark that the $\{\Omega_{i,l},\ 1 \leq i \leq 7,\ l \leq n\}$ are disjoint and that

$$\overline{\Omega} = \left(\bigcup_{l=1}^{n} \bigcup_{i=1}^{7} \overline{\Omega}_{i,l} \right) \cup \overline{\Omega}_{8,n}.$$

We next consider the linear space $S_0^{1,1}(\hat{Q}, \mathcal{T}_{c,m}^{n,\sigma})$. It is spanned by the n nodal basis functions $\{\phi_l\}$ associated to the regular nodes $\{P_l,\ 1 \leq l \leq n\}$ of $\mathcal{T}_{c,m}^{n,\sigma}$. We note that P_l is the node that is common to the elements $\{\Omega_{l,i},\ 1 \leq i \leq 7\}$ at level l; (see Figure 4) and that

$$\begin{aligned} \mathcal{O}_l := supp\,\{\phi_l\} &= \left(\textstyle\bigcup_{i=1}^{7} \overline{\Omega}_{i,l}\right) \cup \left(\textstyle\bigcup_{i=1}^{7} \overline{\Omega}_{i,l+1}\right), \quad 1 \leq l \leq n-1, \\ \mathcal{O}_n := supp\,\{\phi_n\} &= \textstyle\bigcup_{i=1}^{8} \overline{\Omega}_{i,n}. \end{aligned}$$

Let finally $\mathcal{E}(\mathcal{T}_{c,m}^{n,\sigma})$ be the set of all faces e of the elements in $\mathcal{T}_{c,m}^{n,\sigma}$ and, for $e \in \mathcal{E}(\mathcal{T}_{c,m}^{n,\sigma})$, let h_e be the diameter of e.

Our Clément type operator is then defined in the following way.

Definition 7.1 *Given $u \in H_0^1(\hat{Q})$, let*

$$Iu := \sum_{l=1}^{n} a_l\, \phi_l \in S_0^{1,1}(\hat{Q}, \mathcal{T}_{c,m}^{n,\sigma}),$$

where

$$a_l := \frac{\displaystyle\int_{\mathcal{O}_l} u\, dx}{|\mathcal{O}_l|}, \quad 1 \leq l \leq n,$$

and $|\mathcal{O}_l|$ is the volume of $\mathcal{O}_l$.

The following error estimate holds; see [9, Prop. 4.5] for the corresponding two–dimensional result.

Lemma 7.1 *There exists a constant C, that depends on σ but is otherwise independent of $\mathcal{T}^{n,\sigma}_{c,m}$, such that*

$$\sum_{K\in\mathcal{T}^{n,\sigma}_{c,m}} h_K^{-2}\|u-Iu\|^2_{0,K}+\sum_{K\in\mathcal{T}^{n,\sigma}_{c,m}} |u-Iu|^2_{1,K}+\sum_{e\in\mathcal{E}(\mathcal{T}^{n,\sigma}_{c,m})} h_e^{-1}\|u-Iu\|^2_{0,e}\leq C|u|^2_{1,\hat{Q}}.$$

Proof. Given an element $K=\Omega_{i,l}$, of diameter h_K, let ω_K be the union of the supports of the basis functions $\{\phi_l\}$ associated to its nodes. We note that there are at most two such functions. We then have

$$\|Iu\|^2_{0,K}\leq 2\sum_{\mathcal{O}_l\supset K}|a_l|^2\,\|\phi_l\|^2_{0,K}\leq 2\sum_{\mathcal{O}_l\supset K}\frac{|K|}{|\mathcal{O}_l|}\,\|u\|^2_{0,\mathcal{O}_l}\leq 2\sum_{\mathcal{O}_l\supset K}\|u\|^2_{0,\mathcal{O}_l}\leq 4\|u\|^2_{0,\omega_K}. \tag{56}$$

We now define

$$\tilde{u}:=u-|\omega_K|^{-1}\int_{\omega_K}u\,dx.$$

Using (56), we can write

$$\|u-Iu\|_{0,K}=\|\tilde{u}-I\tilde{u}\|_{0,K}\leq 3\|\tilde{u}\|_{0,\omega_K}.$$

Since the diameter of ω_K is comparable to h_K, using the Poincaré inequality, we obtain

$$\|u-Iu\|_{0,K}\leq Ch_K|\tilde{u}|_{1,\omega_K}=Ch_K|u|_{1,\omega_K}, \tag{57}$$

with a constant C that only depends on the shape of ω_K, and thus on σ but not on h_K.

Using an inverse estimate on K, we can write

$$|Iu|_{1,K}=|I\tilde{u}|_{1,K}\leq Ch_K^{-1}\|I\tilde{u}\|_{0,K}\leq Ch_K^{-1}(\|\tilde{u}\|_{0,\omega_K}+\|\tilde{u}-I\tilde{u}\|_{0,K}).$$

By applying the Poincaré inequality on ω_K and (57), we obtain

$$|Iu|_{1,K}\leq C|u|_{1,\omega_K}, \tag{58}$$

with a constant that only depends on σ.

We are now left with the bounds for the face contributions. Given a face $e\subset\partial K$, we can use a trace estimate and obtain

$$h_e^{-1}\|u-Iu\|^2_{0,e}\leq C(h_K^{-2}\|u-Iu\|^2_{0,K}+|u-Iu|^2_{1,K}).$$

We note that the constant C depends on the aspect ratio of K, and thus on σ, but not on h_K. Using (57) and (58), we find

$$h_e^{-1}\|u-Iu\|^2_{0,e}\leq C|u|^2_{1,\omega_K}. \tag{59}$$

The proof is concluded by using (57), (58), and (59) and by summing over the elements. ◻

For the macro–mesh $\mathcal{T}_{c,m}^{n,\sigma}$, we are now ready to prove the following result.

Lemma 7.2 *There exists a constant C, depending on σ, but otherwise independent of $\mathcal{T}_{c,m}^{n,\sigma}$, such that*

$$\inf_{0\neq p\in S_0^{0,0}(\hat{Q},\mathcal{T}_{c,m}^{n,\sigma})} \sup_{0\neq v\in \mathcal{L}_0^{1,1}(\hat{Q},\mathcal{T}_{c,m}^{n,\sigma},)} \frac{(\nabla\cdot v, p)_{\hat{Q}}}{|v|_{1,\hat{Q}}\|p\|_{0,\hat{Q}}} \geq C. \tag{60}$$

Proof. The proof is similar to [9, Th. 4.9] and presented it here for completeness.

We first need to define some local spaces associated to the patches $\{\mathcal{O}_l\}$. For $1 \leq l \leq n$, we set

$$\begin{aligned} S^{0,0}(\mathcal{O}_l) &:= \{p \in L^2(\mathcal{O}_l)|\; p_{|K} \in \mathbb{Q}_0,\; K \subset \mathcal{O}_l\} \\ \mathcal{L}_0^{1,1}(\mathcal{O}_l) &:= \{v \in H_0^1(\mathcal{O}_l)^3|\; v_{|K} \in \mathcal{L}^1(K),\; K \subset \mathcal{O}_l\} \\ N_l &:= \mathbb{Q}_0(\mathcal{O}_l), \end{aligned}$$

and consider the orthogonal decomposition

$$S^{0,0}(\mathcal{O}_l) = N_l \oplus W_l. \tag{61}$$

We then define $\mathcal{E}(\mathcal{O}_l)$ as the set of all interelement faces in $\mathcal{O}_l$ and $\mathcal{E}_0(\mathcal{O}_l)$ as the subset of $\mathcal{E}(\mathcal{O}_l)$ of faces that do not have hanging nodes in their mid–point. Analogous definitions hold for the global sets $\mathcal{E}(\mathcal{T}_{c,m}^{n,\sigma})$ and $\mathcal{E}_0(\mathcal{T}_{c,m}^{n,\sigma})$.

On each patch $\mathcal{O}_l$, we define a mesh–dependent seminorm by

$$|p|^2_{\mathcal{O}_l} := \sum_{e\in\mathcal{E}_0(\mathcal{O}_l)} h_e \int_e |[p]_e|^2 ds, \quad p \in S^{0,0}(\mathcal{O}_l),$$

where $[p]_e$ is the jump of p across a face e. The global seminorm is defined by

$$|p|^2_h := \sum_{e\in\mathcal{E}_0(\mathcal{T}_{c,m}^{n,\sigma})} h_e \int_e |[p]_e|^2 ds,$$

A scaling argument gives, for $p \in W_j$,

$$\sup_{0\neq v\in\mathcal{L}_0^{1,1}(\mathcal{O}_l)} \frac{(\nabla\cdot v, p)_{\mathcal{O}_j}}{|v|_{1,\mathcal{O}_j}} \geq \tilde{\gamma}\; |p|_{\mathcal{O}_j}, \tag{62}$$

with $\tilde{\gamma}$ depending on the shape of $\mathcal{O}_j$, and thus depending on σ but not on h or l.

Given $p \in S_0^{0,0}(\hat{Q}, \mathcal{T}_{c,m}^{n,\sigma})$, we set $p_l := p_{|\mathcal{O}_l}$. According to (61), we have the decomposition

$$p_l = c_l + q_l,$$

where $c_l \in N_l$ is constant and $q_l \in W_l$. The stability condition (62) implies that, for each q_l there exists $v_l \in \mathcal{L}_0^{1,1}(\mathcal{O}_l)$, such that

$$(\nabla \cdot v_l, q_l)_{\mathcal{O}_l} \geq \tilde{\gamma}|q_l|^2_{\mathcal{O}_l}, \quad |v_l|_{1,\mathcal{O}_l} \leq |q_l|_{\mathcal{O}_l},$$

and therefore

$$(\nabla \cdot v_l, p_l)_{\mathcal{O}_l} \geq \tilde{\gamma}|p_l|^2_{\mathcal{O}_l}, \quad |v_l|_{1,\mathcal{O}_l} \leq |p_l|_{\mathcal{O}_l}.$$

If we define $v := \sum_{l=1}^n v_l$, we have

$$(\nabla \cdot v, p)_{\hat{Q}} = \sum_{l=1}^{n} (\nabla \cdot v_l, p)_{\hat{Q}} = \sum_{l=1}^{n} (\nabla \cdot v_l, p_l)_{\mathcal{O}_l} \geq \tilde{\gamma} \sum_{l=1}^{n} |p_l|^2_{\mathcal{O}_l} \geq C|p_l|^2_h,$$

and

$$|v|^2_{1,\hat{Q}} \leq \sum_{l=1}^{n} |v_l|^2_{1,\hat{Q}} \leq C|p_l|^2_h,$$

which are equivalent to

$$\sup_{0 \neq v \in \mathcal{L}_0^{1,1}(\hat{Q}, \mathcal{T}^{n,\sigma}_{c,m})} \frac{(\nabla \cdot v, p)_{\hat{Q}}}{|v|_{1,\hat{Q}}} \geq C_1 |p|_h. \tag{63}$$

We now show that we can replace the seminorm with a norm in (63). The continuous stability condition (3) ensures that for $p \in S_0^{0,0}(\hat{Q}, \mathcal{T}^{n,\sigma}_{c,m})$ there exists $v \in H_0^1(\hat{Q})$, such that

$$(\nabla \cdot v, p)_{\hat{Q}} \geq \gamma \|p\|^2_{0,\hat{Q}}, \quad |v|^2_{1,\hat{Q}} \leq \|p\|^2_{0,\hat{Q}}.$$

We define $u \in S_0^{1,1}(\hat{Q}, \mathcal{T}^{n,\sigma}_{c,m},)^3$ by

$$u_i := I v_i, \quad i = x, y, z.$$

Using integration by parts over the elements, Cauchy–Schwarz, and Lemma 7.1, we find

$$\begin{aligned}
(\nabla \cdot u, p)_{\hat{Q}} &= (\nabla \cdot (u - v), p)_{\hat{Q}} + (\nabla \cdot v, p)_{\hat{Q}} \\
&\geq \sum_{e \in \mathcal{E}_0(\mathcal{T}^{n,\sigma}_{c,m})} \int_e ((u - v) \cdot n)\ [p]_e ds + \gamma \|p\|^2_{0,\hat{Q}} \\
&\geq -\left(\sum_{e \in \mathcal{E}(\mathcal{T}^{n,\sigma}_{c,m})} h_e^{-1} \|u - v\|^2_{0,e} \right)^{1/2} |p|_h + \gamma \|p\|^2_{0,\hat{Q}} \\
&\geq \|p\|^2_{0,\hat{Q}} \left(C_3 - C_2 \frac{|p|_h}{\|p\|_{0,\hat{Q}}} \right).
\end{aligned}$$

Since $|u|_{1,\hat{Q}} \leq C\|p\|_{0,\hat{Q}}$, we have

$$\sup_{0\neq u\in\mathcal{L}_0^{1,1}(\hat{Q},\mathcal{T}_{c,m}^{n,\sigma})} \frac{(\nabla\cdot u,p)_{\hat{Q}}}{|u|_{1,\hat{Q}}} \geq \|p\|_{0,\hat{Q}} \left(C_4 - C_5\frac{|p|_h}{\|p\|_{0,\hat{Q}}}\right). \quad (64)$$

Combining (63) and (64), we then have

$$\sup_{0\neq v\in\mathcal{L}_0^{1,1}(\hat{Q},\mathcal{T}_{c,m}^{n,\sigma})} \frac{(\nabla\cdot v,p)_{\hat{Q}}}{|v|_{1,\hat{Q}}} \geq \|p\|_{0,\hat{Q}} \min_{t\geq 0} f(t),$$

with $t := |p|_h/\|p\|_{0,\hat{Q}}$ and $f(t) := \max\{C_4 - C_5 t, C_1 t\}$. The proof is concluded by noticing that $\min_{t\geq 0} f(t) = (C_1C_4)/(C_1+C_5) > 0$. □

We then obtain the following stability result for corner patches, by using Lemma 7.2 and noticing that the anisotropically refined elements in $\mathcal{T}_{c,m}^{n,\sigma}$ are particular face and edge patches.

Theorem 7.1 *Let $\mathcal{T}_c$ be a corner patch with grading factor σ and n layers. Then, there exists a constant C, that depends on σ, but is independent of k, n, and the aspect ratio of $\mathcal{T}_c$, such that*

$$\inf_{0\neq p\in S_0^{k-2,0}(\hat{Q},\mathcal{T}_c)} \sup_{0\neq v\in S_0^{k,1}(\hat{Q},\mathcal{T}_c)^3} \frac{(\nabla\cdot v,p)_{\hat{Q}}}{|v|_{1,\hat{Q}}\|p\|_{0,\hat{Q}}} \geq Ck^{-1}. \quad (65)$$

Proof. It is enough to use Theorem 4.1 with $\mathcal{T} = \mathcal{T}_c$ and $\mathcal{T}_m = \mathcal{T}_{c,m}$. □

8 Stability of geometric edge meshes

We now consider the case of geometric edge meshes $\mathcal{T} = \mathcal{T}_{edge}^{n,\sigma}$, introduced in Section 3.2. In a similar way as before, we employ a macro–element technique, described in Figure 2.

At the top level, we have the shape–regular macro–mesh $\mathcal{T}_m$, which is successively refined, either isotropically, or anisotropically towards an edge (second level, left) or a corner (second level, right). The divergence stability for the shape–regular macro–mesh at the top level and the isotropically refined patches is proven in [14]. We then need to prove the stability of the single patches for the higher order spaces.

8.1 Edge patches

For an edge patch, the same analysis for the case of a boundary layer mesh in Section 6 can be carried out here. Indeed, an edge patch is given by a mesh $\mathcal{T}_e$ of the form (8), where the two–dimensional triangulation $\mathcal{T}_{xy}$ is an irregular corner mesh, with grading factor σ and n layers. The following theorem holds.

Theorem 8.1 *Let $\mathcal{T}_e$ be an edge triangulation with grading factor σ and n layers. Then, there exists a constant C, that depends on σ, but is independent of k, n, and the aspect ratio of $\mathcal{T}_e$, such that*

$$\inf_{0\neq p\in S_0^{k-2,0}(\hat{Q},\mathcal{T}_e)} \sup_{0\neq v\in S_0^{k,1}(\hat{Q},\mathcal{T}_e)^3} \frac{(\nabla\cdot v,p)_{\hat{Q}}}{|v|_{1,\hat{Q}}\|p\|_{0,\hat{Q}}} \geq Ck^{-1}. \tag{66}$$

Proof. We use a macro–element technique; $\mathcal{T}_e$ itself plays the role of macro–mesh. The stability for the low–order, two–dimensional spaces $S_0^{2,1}(\hat{S},\mathcal{T}_{xy})^2$ and $S_0^{0,0}(\hat{S},\mathcal{T}_{xy})$ is proven in [9, Sect. 4]. Then, there exists an operator π_{xy} that also satisfies (53), with a constant C that only depends on σ. Using π_{xy}, we can prove Lemma 6.3 in exactly the same way as for boundary layer meshes, and this ensures that the low–order spaces $S_0^{2,1}(\hat{Q},\mathcal{T}_e)^2$ and $S_0^{0,0}(\hat{Q},\mathcal{T}_e)$ are divergence stable, with a constant that only depends on σ but is otherwise independent of n and the diameter and the aspect ratio of $\mathcal{T}_e$.

The existence of a Fortin operator that satisfies Corollary 5.2 and the inf–sup condition (3) for the continuous spaces ensure that the inf–sup condition for the local spaces $S_0^{k,1}(K)^3$–$S_0^{k-2,0}(K)$ holds with a constant γ_N that is bounded from below by Ck^{-1}, and is independent of the diameter and the aspect ratio of $K\in\mathcal{T}_e$.

The proof is concluded by applying Theorem 4.1 with $\mathcal{T}=\mathcal{T}_e$ and $\mathcal{T}_m=\mathcal{T}_e$. □

8.2 Corner patches

For a corner patch, the analysis is similar to that in Section 7. A corner patch is given by a mesh $\mathcal{T}_c$ obtained by refining an initial irregular corner mesh $\mathcal{T}_{c,m}$ towards the edges only. The following theorem holds.

Theorem 8.2 *Let $\mathcal{T}_c$ be a corner patch with grading factor σ and n layers. Then, there exists a constant C, that depends on σ, but is independent of k, n, and the aspect ratio of $\mathcal{T}_c$, such that*

$$\inf_{0\neq p\in S_0^{k-2,0}(\hat{Q},\mathcal{T}_c)} \sup_{0\neq v\in S_0^{k,1}(\hat{Q},\mathcal{T}_c)^3} \frac{(\nabla\cdot v,p)_{\hat{Q}}}{|v|_{1,\hat{Q}}\|p\|_{0,\hat{Q}}} \geq Ck^{-1}. \tag{67}$$

Proof. We use a macro–element technique with $\mathcal{T}_{c,m}$ as macro–mesh. The macro–mesh $\mathcal{T}_{c,m}$ is the same as in the case of boundary layer meshes and, consequently, Lemma 7.2 holds.

The proof is concluded by noticing that the anisotropically refined elements in $\mathcal{T}_{c,m}$ are particular edge patches and by using Theorem 4.1 with $\mathcal{T}=\mathcal{T}_c$ and $\mathcal{T}_m=\mathcal{T}_{c,m}$. □

References

[1] Mark Ainsworth and Patrick Coggins. The stability of mixed *hp*–finite element methods for Stokes flow on high aspect ratio elements. *SIAM J. Numer. Anal.*, 38(5):1721–1761, 2000.

[2] B. Andersson, U. Falk, I. Babuška, and T. von Petersdorff. Reliable stress and fracture mechanics analysis of complex aircraft components using a *hp*–version FEM. *Int. J. Numer. Meth. Eng.*, 38(13):2135–2163, 1995.

[3] Ivo Babuška and Benqi Guo. Approximation properties of the *hp*–version of the finite element method. *Comp. Methods Appl. Mech. Eng.*, 133:319–346, 1996.

[4] Christine Bernardi and Yvon Maday. Spectral methods. In *Handbook of Numerical Analysis, Vol. V, Part 2*, pages 209–485. North-Holland, Amsterdam, 1997.

[5] Franco Brezzi and Michel Fortin. *Mixed and Hybrid Finite Element Methods*. Springer-Verlag, New-York, 1991.

[6] Jens Markus Melenk. On robust exponential convergence of finite element methods for problems with boundary layers. *IMA Journal of Numerical Analysis*, 17:577–601, 1997.

[7] Dominik Schötzau. *hp-DGFEM for parabolic evolution problems*. PhD thesis, ETH Zürich, 1999.

[8] Dominik Schötzau and Christoph Schwab. Mixed *hp*-FEM on anisotropic meshes. *Math. Models Meth. Appl. Sci.*, 8:787–820, 1998.

[9] Dominik Schötzau, Christoph Schwab, and Rolf Stenberg. Mixed *hp*–FEM on anisotropic meshes II: Hanging nodes and tensor products of boundary layer meshes. *Numer. Math.*, 83:667–697, 1999.

[10] Christoph Schwab. *p– and hp– finite element methods*. Oxford Science Publications, 1998.

[11] Christoph Schwab and Manil Suri. The *p* and *hp* version of the finite element method for problems with boundary layers. *Math. Comp.*, 65:1403–1429, 1996.

[12] Christoph Schwab, Manil Suri, and Christos A. Xenophontos. The *hp*–FEM for problems in mechanics with boundary layers. *Comp. Methods Appl. Mech. Eng.*, 157:311–333, 1998.

[13] Rolf Stenberg. Error analysis of some finite element methods for Stokes problem. *Math. Comp.*, 54:495–508, 1990.

[14] Rolf Stenberg and Manil Suri. Mixed *hp* finite element methods for problems in elasticity and Stokes flow. *Numer. Math.*, 72:367–389, 1996.

Research Reports

No.	Authors	Title
01-02	A. Toselli, C. Schwab	Mixed *hp*-finite element approximations on geometric edge and boundary layer meshes in three dimensions
01-01	A. Buffa, M. Costabel, C. Schwab	Boundary element methods for Maxwell's equations on non-smooth domains
00-18	B.Q. Guo, C. Schwab	Analytic regularity of Stokes flow in polygonal domains
00-17	M.H. Gutknecht, S. Röllin	Variations of Zhang's Lanczos-Type Product Method
00-16	M.H. Gutknecht, S. Röllin	The Chebyshev iteration revisited
00-15	G. Schmidlin, C. Schwab	Wavelet Galerkin BEM on unstructured meshes by aggregation
00-14	B. Cockburn, G. Kanschat, D. Schötzau, C. Schwab	Local Discontinuous Galerkin methods for the Stokes system
00-13	O. Bröker, M.J. Grote, C. Mayer, A. Reusken	Robust Parallel Smoothing for Multigrid Via Sparse Approximate Inverses
00-12	C. Lasser, A. Toselli	An overlapping domain decomposition preconditioner for a class of discontinuous Galerkin approximations of advection-diffusion problems
00-11	J. Liesen, M. Rozložník, Z. Strakoš	On Convergence and Implementation of Minimal Residual Krylov Subspace Methods for Unsymmetric Linear Systems
00-10	C. Schwab, O. Sterz	A scalar boundary integrodifferential equation for eddy current problems using an impedance boundary condition
00-09	M.H. Gutknecht, M. Rozložník	By how much can residual minimization accelerate the convergence of orthogonal error methods?
00-08	M. Rozložník, V. Simoncini	Short-term recurrences for indefinite preconditioning of saddle point problems
00-07	P. Houston, C. Schwab, E. Süli	Discontinuous *hp*-Finite Element Methods for Advection-Diffusion Problems
00-06	W.P. Petersen	Estimation of Weak Lensing Parameters by Stochastic Integration
00-05	M.H. Gutknecht	A Matrix Interpretation of the Extended Euclidean Algorithm
00-04	M.J. Grote	Nonreflecting Boundary Conditions for Time Dependent Wave Propagation
00-03	M.H. Gutknecht	On Lanczos-type methods for Wilson fermions